Energy 234 (2021) 121200

Contents lists available at ScienceDirect

Energy

journal homepage: www.elsevier.com/locate/energy

Thermal energy storage sizing for industrial waste-heat utilization in district heating: A model predictive control approach

Brage Rugstad Knudsen*, Daniel Rohde, Hanne Kauko

SINTEF Energy Research, Kolbjørn Hejes vei 1B, Trondheim, 7491, Norway

ARTICLE INFO

Article history:
Received 21 December 2020
Received in revised form
1 June 2021
Accepted 5 June 2021
Available online 15 June 2021

Keywords:
Thermal energy storage
Waste-heat utilization
District heating
Model predictive control

ABSTRACT

Thermal energy storage (TES) is a key technology for enabling increased utilization of industrial waste heat in district heating. The ability of TES to equalize offsets in demand and supply depends strongly on the sizing, control and integration in a heating plant. We consider the problem of sizing TES in heating plants utilizing a varying waste-heat source. To this end, we propose a combined dynamic simulation and model predictive control approach that accounts for the dynamics and optimal control of the heating plant with TES. A case study has been carried out on a district-heating plant located in Norway, with 90% of its annual heat production being heat recovered from the off-gas from a ferrosilicon plant. We evaluate the effective peak-heating reduction with different TES sizes and the energy-to-heat-flow-ratio for the TES discharging periods as performance metrics. For the case study, our results suggest that a modest TES tank volume of 1500 m^3 is sufficient to achieve a half-year peak-heating reduction of 12% and comparable performance with larger volumes. The proposed methodology constitutes a numerically tractable means of incorporating the impact of model predictive control on the sizing of TES for heating plants with time-varying waste-heat supply and demand.

1. Introduction

Utilization of industrial and urban waste heat sources in district-heating networks (DHNs) has a great potential to contribute to the replacement of fossil fuel based heating in Europe and globally, and thus to achieving 2050 climate goals [1]. Previous studies have quantified the abundance of industrial waste heat [2] and its potential for utilization for district heating (DH) [3]. Effective utilization of industrial waste heat is, however, challenging for several reasons: (i) The available waste heat may be highly time varying, both in temperature and heat-flow rate; (ii) The waste heat may be offset with the buildings' heating demands; and (iii) The distance between the waste-heat source and the consumers may be long. Even if the available waste heat in many cases exceeds the DH demand, DH operators may still need significant shares of peak heating during periods of high demand, increasing the costs and often emissions related to the heat production. To improve utilization of varying waste-heat sources in DHNs and thereby reduce the use of peak-heating sources, thermal energy storage (TES) is a key technology.

This study focuses on the sizing of centralized short-term TES for DH systems with varying, uncontrollable waste-heat sources. For this purpose, the most common type of TES is a large, pressurized hot-water tank [4], often enabling a suitable temperature range for conventional high-temperature DH [5], while being a well-known and robust technology. The cost of installing a TES unit may, however, be significant and the space available at the heating plant may be limited. Moreover, the optimal size of TES for waste-heat utilization in DH depends both on the heat availability, its time variations and how it matches the demand. An oversized TES may impede efficient utilization of the available waste heat due to increased charging time and heat losses [6]. Long charging times reduces the ability a short-term TES offers to quickly react to and compensate for offsets between available waste heat and the demand. Too small volumes, on the other hand, will lead to frequent temperature saturation of the TES and hence higher rejection of waste heat, as well as rapid discharge, and thus an increased demand for peak heating. Additionally, the control of the heating plant and the TES may greatly affect the degree of waste-heat utilization in cases with large mismatch in demand and supply. These operational conditions may significantly impact the optimal size of a TES, and are often little accounted for or neglected during sizing

* Corresponding author.
E-mail address: brage.knudsen@sintef.no (B.R. Knudsen).

https://doi.org/10.1016/j.energy.2021.121200

evaluations due to the different time scales of the control and payback horizon of the investment [7]. This paper contributes to the extant litterateur (reviewed below) on this challenge by presenting a sizing scheme based on comprehensive dynamic system simulations and model predictive control (MPC) of a heating plant, applied to case study of a DH plant in an Norwegian industry cluster with time-varying waste heat as the main heat source.

1.1. Literature review

Sizing of TES has been addressed in a number of previous studies by different approaches. Cao and Cao [8] evaluated simple optimization methods for sizing of TES in boiler plants in industrial facilities based solely on the load graph. Labidi et al. [9] used an iterative, parametric approach based on a steady-state energy balance to size a TES unit for multi-energy district boilers, with subsequent simulations of the operational strategy. Kauko et al. [10] used similarly an iterative, steady-state approach based on energy balances to evaluate the payback period and the reduction in emissions as a function of TES size. These methods for sizing of TES do, however, only consider the heat amount and not the temperature levels, and hence may overestimate the achievable performance of the TES. Badami et al. [11] developed an integrated dynamic thermo-fluid tool with Monte-Carlo simulations for design of DHNs with the possibility to add distributed TES units in the network. Kyriakis and Younger [12] considered hot-water tanks coupled with geothermal energy for use in DH, for which they proposed a two-stage approach with optimized system design in the first stage and analysis of the daily and annual operations in the second stage. Pinnau and Breitkopf [13] developed a methodology for sizing of TES for buildings based on Fourier analysis of heat-load profiles, using a ratio of the thermal power and storage capacity as the design requirement. In a related approach, Stalinski and Duquette [14] used fast Fourier transform to decompose a set of system residual heating profiles generated from a TRNSYS TES model to determine an optimal storage volume.

Combined heat and power (CHP) plants have spurred significant research into optimal sizing of TES. Caliano et al. [15] considered design optimization of biomass-fired combined heat, cooling and power (CHCP) with TES by optimizing different plant configurations with TES over a fixed 5-year payback period. Sartor and Dewallef [16] investigated the design and integration of a central TES system in a biomass CHP plant, with controllable load of the biomass plant. They applied thermodynamic simulations with a steady-state network model and a simple TES charging and discharging control strategy to evaluate the optimal sizing of the TES and the corresponding payback period. Urbanucci et al. [17] proposed a two-level design and operational optimization approach for CHP plants with TES. The upper-level problem found optimal size and thermal capacity for the TES that minimized the annualized investment cost, while a rolling-horizon mixed integer linear programming (MILP) model optimized the operation of the system with a simplified system model. Besides the aforementioned approaches, studies on optimal sizing and operations of CHP or CHCP plats with TES often resort to planning models with MILP, e.g. Pérez-Iribarren et al. [18]; using cost-capacity curves or static models of the TES with a representative days approach and no detailed description of the control or dynamic interactions with the heat sources.

Compared with sizing of TES with controllable heat sources, both the time-variations of the waste heat and the demand must be accounted for to adequately size a TES with uncontrollable sources. To address this challenge, Simeoni et al. [19] developed a cost-type multi-objective optimization model for evaluating an energy system receiving waste heat from an industrial facility to supply heat to a DHN. The capacity of the TES was optimized to fulfill the heat demand, but no dynamics of the heating plant were included. In a similar vein, Simeoni et al. [20] evaluated cold and hot TES for a centralized CHCP plant with different waste-heat sources in a food industry cluster in Italy. Li et al. [21] considered combined short-term and borehole TES for a campus DH receiving waste heat from a data centre, using a regression cost curve and a desired capacity for the sizing of the storages. Sizing of TES for waste-heat utilization in DH resembles the challenge of sizing of electric storage with integration of intermittent renewables. For instance, Alnaser et al. [22] proposed a two-stage iterative approach to minimize storage size by means of energy and power output to reduce curtailment of electricity from a wind farm. Approaches for optimally sizing electrical storage for integration of intermittent renewables tend to use energy and power or ratios relative to the number of charging and discharging cycles over a desired time horizon for the storage, see e.g. Das et al. [23]. Hence, such approaches are akin to the approach of, e.g., Pinnau and Breitkopf [13]; and do not account for thermal inertia effects and dynamic interactions of the TES with the heating plant.

Tarragona et al. [24] concluded in a recent bibliographic review on smart control applications for TES systems, including MPC, that one of the gaps in the literature is optimized sizing approaches that incorporates MPC in the evaluation of different storage sizes. Yet, a few works in this field exist. Jonin et al. [25] constructed an exergy-based MPC scheme for a building with seasonal TES receiving heat from a solar collector. They evaluated the control scheme for different tank sizes to find a suitable volume that prevented violation of the temperature supply requirements. D'Ettorre et al. [26] developed an MPC scheme for hybrid heat-pump and thermal-storage systems in buildings with evaluation of cost-effective sizing relative to the MPC prediction horizon. Thombre et al. [27] compared two approaches for optimizing the capacity of a TES subject to demand uncertainty with incorporation of operational constraints. The approach, however, did not account for temperature variations and was based on extrapolation with a representative week to allow evaluation over a 5-year time horizon.

1.2. Contribution

In light of the reviewed literature, there is a lack of sizing approaches for TES that account for both optimal control and the system dynamics of the DH plant as a part of assessing the achievable performance with installation of TES. Not accounting for these aspects may lead to suboptimal sizing of the TES units [26], and thus excessive use of peak heating sources, increasing the costs and emissions of the heat production. Moreover, there is a gap in approaches that analyze the trade-off between storage capacity and achievable heat-flow rate (thermal power) in sizing of a TES unit, taking into account temperature variations in the TES and the output to the DHN, and how this ratio varies over time and operation of the heating plant. This paper contributes to the gap of such approaches by presenting a scheme for analyzing TES sizing at DH plants with industrial waste-heat utilization through the use of MPC and detailed dynamic system simulations. The attractiveness of MPC for TES sizing comes from the possibility to ensure tight satisfaction of historical data on available waste heat, demand and temperatures. Furthermore, by being an optimal-control scheme, MPC provides a means of evaluating the maximum achievable operational performance with installation of TES. The TES discharge energy-to-heat-flow ratio is introduced as a metric for comparing the utilization of different sized TES relative to the waste-heat availability and the demand. We apply the proposed scheme to a real case study for the DH plant of Mo District Heating outside Mo i Rana, Norway.

The remainder of the paper is organized as follows. Section 2 presents the case study. Section 3 describes the proposed sizing methodology. In Section 4, we present numerical results from the case study with discussions in Section 5 and conclusions in Section 6.

2. Case study

Mo District Heating supplies heat to the citizens of Mo i Rana, Norway, with the heating plant located in Mo Industry Park. Mo District Heating recovers heat from the off-gas from the Elkem Rana ferrosilicon plant, with an annual heat production of 85–90 GWh of which about 90% comes from the off-gas waste-heat recovery.

Fig. 1 shows the human machine interface (HMI) of the heating plant. The two boilers 5 and 6 transfer heat from the off-gas to the DHN, and have a total capacity of 22 MW and a maximum output temperature of 120°C. The operator has four peak-heating boilers with a total capacity of 21 MW, displayed as boilers 1–4 in Fig. 1, running on CO-gas obtained as a by-product from a manganese plant in the industry park, electricity or oil (as back-up), respectively. All the boilers are equipped with energy meters. The heat supply is controlled by outdoor temperature compensation. Peak heating is applied whenever the temperature obtained from boiler 5 and 6 drops below the desired supply temperature level, and the decision on which peak-heating boiler to switch on depends on the electricity price and availability of CO gas. While the two oil boilers have historically constituted a marginal share of the heating mix,[1] an environmental objective is to eliminate the use of oil in the heat production.

The available waste heat for the period from January 1, 2018 to May 1, 2019, is shown in Fig. 2 together with the heat demand of the DHN in Mo i Rana. Total peak heating and dumped heat for the same period are shown in Fig. 3. The annual amount of available waste heat exceeds the heat demand by far, but time variations and offsets in heat availability and demand causes a need for peak heating. The overall peak-heating use is comparably low, but constitutes a significant share of both the costs and emissions related to the heat production.

A large share of the dumped heat, that is, waste heat that is not utilized for DH, is available in months with low demand as seen in Fig. 3. This waste heat is difficult to utilize without high-temperature seasonal TES. Yet, from Fig. 3, it can be observed that heat is rejected also during winter months with high demand. Changes in boiler equipment early in 2018 and unusual cold weather caused extensive peak heating and relatively low heat dumping during the winter of 2018. For this period, the potential of short-term TES to reduce peak heating was thus limited. For our study, we have therefore considered the time window from November 2018 through April 2019.

3. Methodology

In this section, we describe the proposed methodology for detailed TES sizing assessment in DH plants with waste-heat utilization. The methodology relies on iterative, parametric evaluation of different TES volumes in a predefined set $\mathscr{V}^{\text{TES}}$ over a chosen evaluation period $E^{\text{TES,eval}}$, with optimization of control inputs for the heating plant and TES using MPC and subsequent dynamic simulations. We have used a hot-water tank as TES. The work flow for the proposed scheme is shown in Fig. 4. The main component in the work flow is a dynamic system model of the heating plant used for simulations in Step 1 and 3, and in the MPC in Step 2. In Step 1, the heating plant without TES was first simulated over the time horizon $E^{\text{TES,eval}}$ using available measurement data of the control inputs. This was done to identify any inconsistencies or outliers in the measurement data, fill in possible missing data points in the time series, and by this generate a consistent base case for evaluation of different TES tank volumes. The base case was also used together with the measurement data to generate demand predictions for the MPC as shown in Fig. 4. Below, we describe the dynamic model of the heating plant, the MPC scheme, the numerical implementation, and the chosen metrics to evaluate the impact of a TES with a given volume. Sets and indices used in the model are provided in Table 1.

3.1. Dynamic model of the heating plant

A dynamic model of the heating plant at Mo District Heating depicted in Fig. 1 has been developed using the modeling language Modelica [28]. Modelica is object oriented, providing high modularity and adaptability of the created component models, and has been proven to be an efficient modeling language for analysis and optimization of thermal energy systems, e.g. Schweiger et al. [29].

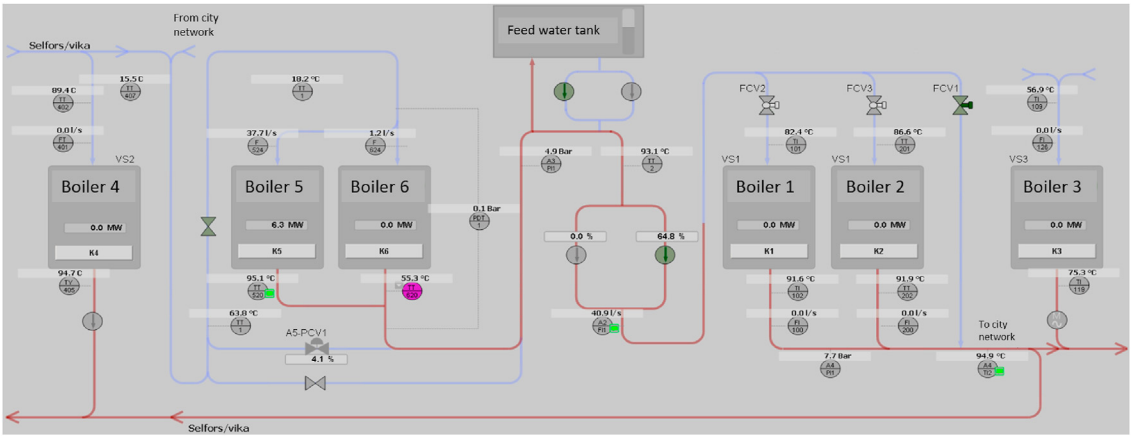

Fig. 1. Human machine interface of the heating plant at Mo Disctrict Heating.

[1] https://www.fjernkontrollen.no/mo-fjernvarme/.

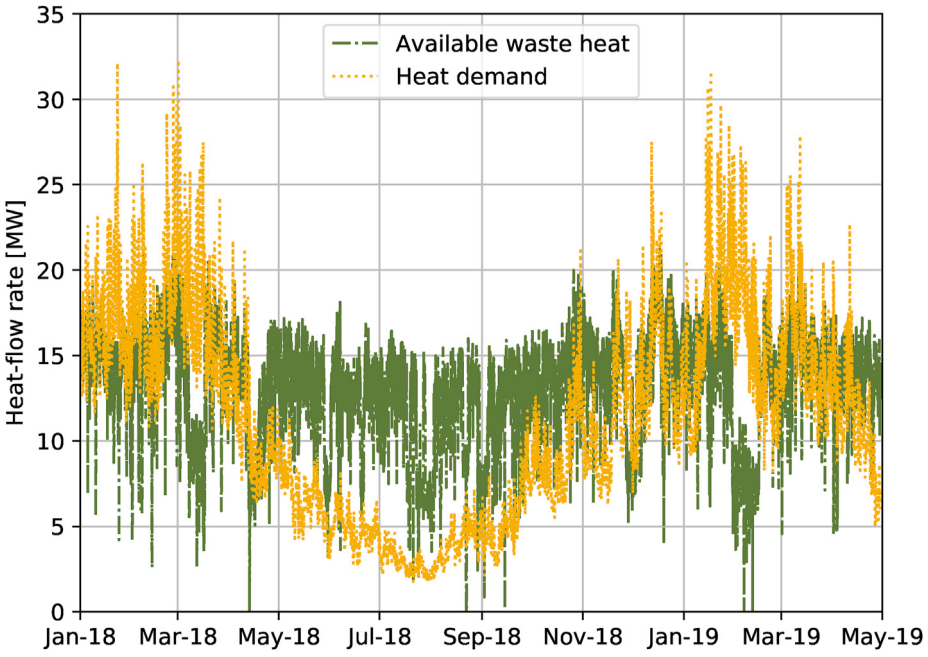

Fig. 2. Waste-heat availability and district-heating demand for Mo District Heating for the period from January 1, 2018 to May 1, 2019. For the case study, we have considered the time window from November 2018 through April 2019.

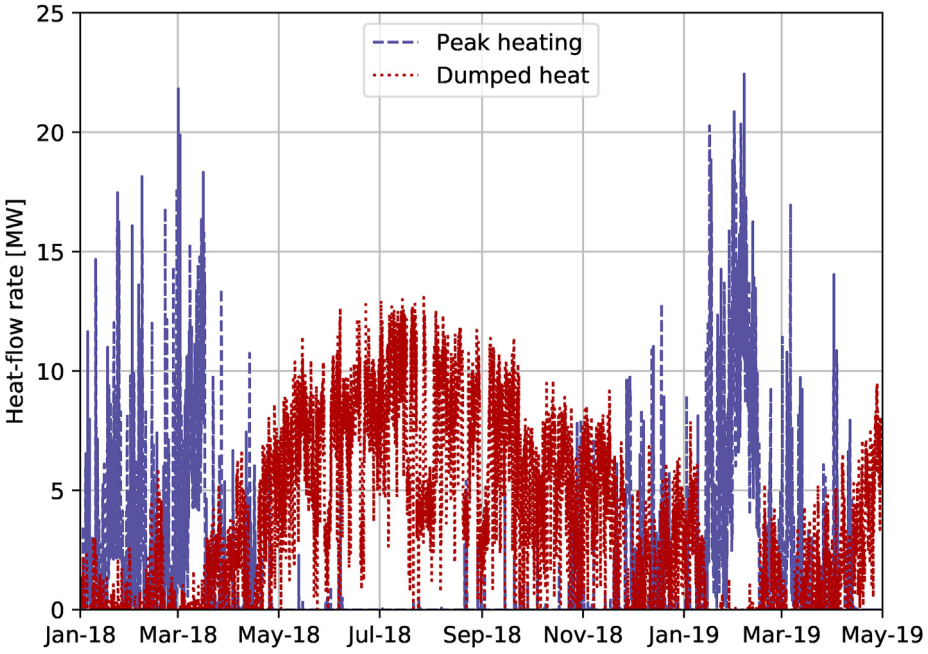

Fig. 3. Dumped heat from boiler 5 and 6 in the heating plant of Mo District Heating displayed in Fig. 1, together with the sum of peak heating from boiler 1–4 for the period from January 1, 2018 to May 1, 2019. For the case study, we have considered the time window from November 2018 through April 2019.

Fig. 5 shows the Modelica model of the heating plant extended with a TES. The system boundary of the heating-plant model is the return and supply line of the DHN, i.e. the grid itself was not modeled. Space limitations and physical constraints of the off-gas heat-recovery process impede heat recovery directly to the TES upstream of boiler 5 and 6. Consequently, the TES tank is connected downstream of boiler 5 and 6 in the model and charged by increasing the heat uptake in the boilers, feeding the excess heat into the TES. The mass-flow rates of the circulation pumps and the heat-flow rate for the peak heating were selected as control inputs in the model.

The boilers were modeled as lumped fluid volumes. Boilers 1–4 in Fig. 1 were lumped into one fluid volume model, as the scope of the heating-plant model was to analyze possible reduction in peak heating with TES, without differentiating between the different peak-heating sources. The heat-recovery heat exchanger in these boilers was modeled based on the effectiveness-NTU method [30]. Due to lack of heat-exchanger design details, the effectiveness was not calculated based on a correlation. Instead, a constant value

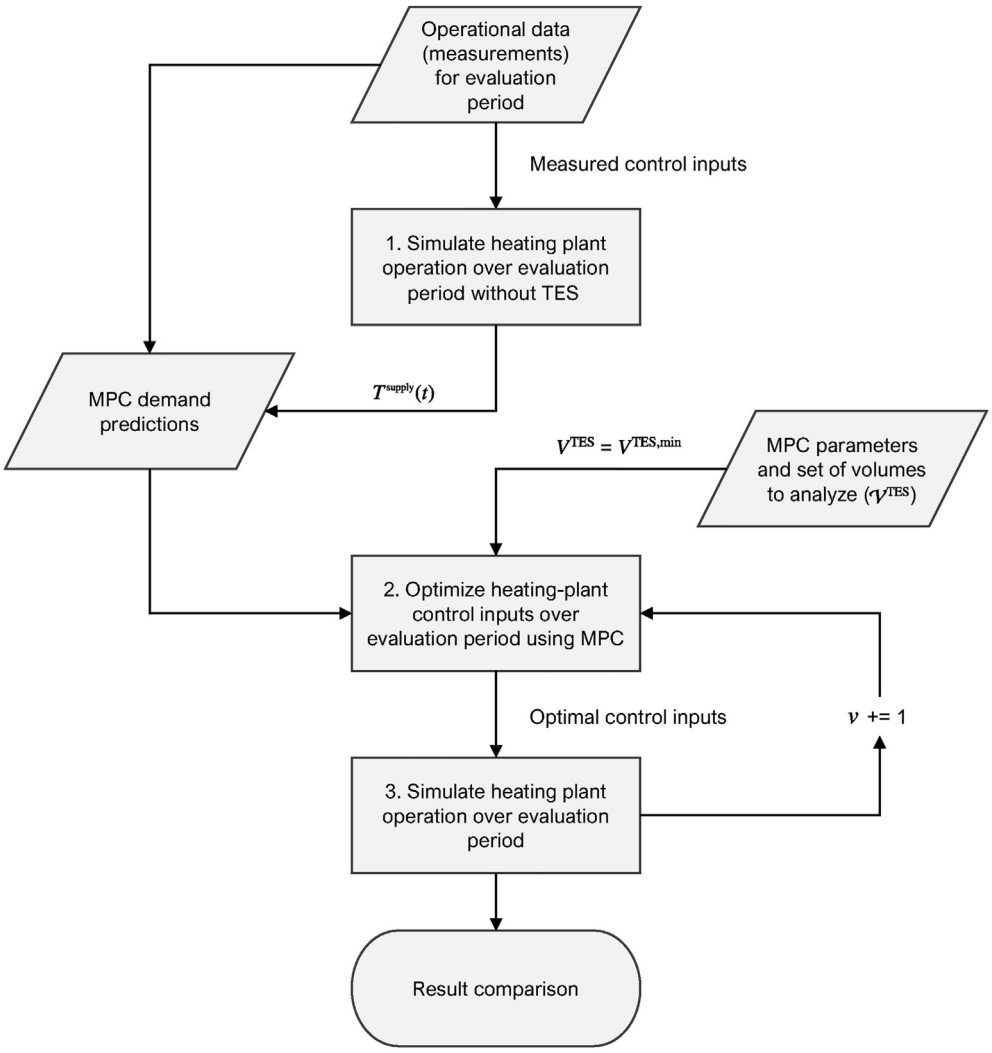

Fig. 4. Work flow of the proposed simulation and MPC based TES sizing methodology.

Table 1
Sets and indices.

Index	Interpretation	Set	Elements
i	Heat-recovery boiler	$\mathcal{I}$	{b5, b6}
j	Controlled pumps	$\mathcal{J}$	{b5, b6, bypass, TES-charge, TES-discharge}
t_k	Samples of the MPC controller	$\mathcal{T}$	$\{t_0, t_1, \ldots\}$
k	Discharge periods of the TES	$\mathcal{T}^{dc}$	{1, 2, …}
v	Set of tank volumes analyzed	$\mathcal{V}^{TES}$	$\{V^{TES,min}, \ldots, V^{TES,max}\}$

based on the measured operation data was chosen, set to 0.52 and 0.58 for boilers 5 and 6, respectively.

The TES tank was modeled as coupled fluid volumes, representing horizontal fluid layers in the tank. Each of these layers were assumed to have uniform temperature, and internal heat exchange between the layers was neglected. The volume of one fluid volume was set to 100 m^3, thus the number of layers depended on the given tank volume. The fluid layers were thermally connected to the ambient with a size-dependent UA-value, and heat losses to the ambient were calculated using historical data for ambient temperature for the region in the considered period. The UA value was calculated by multiplying the surface area of the cylindrical tank with a heat transfer coefficient of 0.25 W/(m2K). Heat losses from the boilers and connecting pipes were neglected.

The flow inside the tank was assumed to be one-dimensional, from top to bottom during charging and from bottom to top during discharging. This possibility for flow reversal is challenging in the numerical optimization of the control inputs in Step 2 as it requires incorporating switching decision in the optimization problem; see e.g. Biegler [31]; Ch. 11). To circumvent this problem, a complementary tank model was developed and incorporated in the model used for the control-input optimization in Step 2 of Fig. 4. In this model, the tank was divided into two vertical segments, in addition to the horizontal discretization described above. Thus, each horizontal layer consisted of two fluid volumes (each containing 50 m^3), which allowed to separate charging and discharging

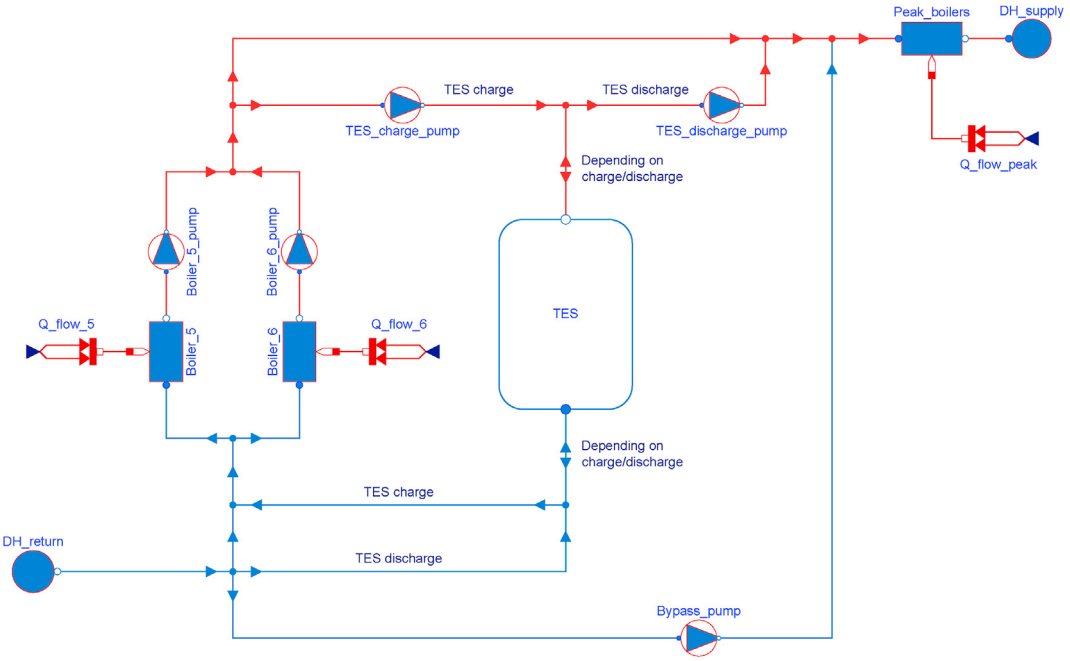

Fig. 5. Simplified schematic of the heating plant model in Dymola (HMI shown in Fig. 1).

flow. Ideal heat transfer was assumed ($R \ll 1$ K/W) between the two fluid volumes in each layer. This led to the same TES capacity of the complementary tank model used in the optimization and similar heating-plant behavior as the model used in the simulations.

3.2. Model predictive control scheme

In Step 2 of the sizing methodology, MPC was used to compute optimal control-inputs to the heating-plant model. The MPC iteratively solves an optimal-control problem (OCP) that incorporates the heating-plant model described in Section 3.1, heat-demand and waste-heat predictions, and constraints on the control inputs, states and algebraic variables in the model. The implemented set-up of the MPC controller used the in current study is as follows. At each sampling instant $t_k \in \mathcal{T} := \{t_0, t_1, \ldots\}$ of the MPC controller, demand predictions for the DHN by means of heat-flow rate $\hat{Q}^{\mathrm{DH}}(t)$ and supply temperature $\hat{T}^{\mathrm{DH}}(t)$ for the time horizon $t \in [t_k, t_k + \Delta_t]$, with Δ_t as fixed prediction horizon, were provided to the controller. Additionally, predictions $\hat{T}^{\mathrm{return}}(t), t \in [t_k, t_k + \Delta_t]$ of the return temperature to the heating plant was provided to the controller. Such predictions would typically be computed from the mass-flow rate and heat demand in the DHN up to the current sampling time t_k together with knowledge on the dominating time-delay in the grid, see e.g. Geysen et al. [32] and Guelpa et al. [33]. To enforce satisfaction of the demand, we have adopted the formulation in Knudsen et al. [34] and imposed the constraints

$$\hat{T}^{\mathrm{DH}}(t) - \alpha \leq T^{\mathrm{supply}}(t) \leq \hat{T}^{\mathrm{DH}}(t) + \alpha, \tag{1a}$$

$$\hat{Q}^{\mathrm{DH}}(t) \leq Q^{\mathrm{supply}}(t) \leq (1+\beta)\hat{Q}^{\mathrm{DH}}(t). \tag{1b}$$

Here, α is a non-negative parameter that was added to allow small deviations between the provided and demanded DH supply temperature, and $\beta \in [0, 0.05]$ similarly an allowed upper deviation on delivered heat. $T^{\mathrm{supply}}(t)$ and $Q^{\mathrm{supply}}(t)$ are the supply temperature and heat-flow rate to the DH network in the heating-plant model, respectively, with

$$Q^{\mathrm{supply}}(t) = \dot{m}^{\mathrm{DH}}(t) c_{\mathrm{p}} \left(T^{\mathrm{supply}}(t) - \hat{T}^{\mathrm{return}}(t) \right) \tag{2}$$

In (2), $\dot{m}^{\mathrm{DH}}(t)$ is the mass-flow rate of the supply to the DHN. Exact satisfaction of demand by means of imposing equality constraints is numerically challenging due to the thermal inertia in the system and the overall optimization problem being nonlinear. Allowing the small slack in the demand constraints (1) thus improves the numerical robustness. As a simplified scheme for control of the waste-heat recovery, we have implemented the following setup: At each sample t_k, the MPC was provided with predictions of the available waste heat $\hat{Q}^{\mathrm{WH},i}(t), i \in \mathcal{I}$ for $t \in [t_k, t_k + \Delta_k]$ based on the plant measurement data. The MPC controller was allowed to utilize heat up to this maximum available heat-flow rate $\hat{Q}^{\mathrm{WH},i}(t)$, either for covering the DHN demand or for charging the TES. Any residual waste heat that was not recovered by the boilers was dumped, modeled with the constraints

$$Q^{\mathrm{WHtoDH},i}(t) + Q^{\mathrm{dump},i}(t) = \hat{Q}^{\mathrm{WH},i}(t), i \in \mathcal{I}, \tag{3a}$$

$$Q^{\mathrm{dump},i}(t) \geq 0, i \in \mathcal{I}, \tag{3b}$$

where $Q^{\mathrm{dump},i}$ is heat dumped for boiler 5 and 6, respectively. The control inputs, $u(t) = [Q^{\mathrm{peak}}(t), Q^{\mathrm{dump},i}(t), \dot{m}(t)']'$, where $\dot{m}(t)'$ is a vector with the mass-flow rates of the five controllable pumps in Fig. 5, were subject to the bound constraints

$$0 \leq \dot{m}^{j}(t) \leq \dot{m}^{\mathrm{max},j}(t), j \in \mathcal{J}, \tag{4a}$$

$$0 \leq Q^{\mathrm{peak}}(t), \tag{4b}$$

where $\dot{m}^{\mathrm{max},j}(t)$ is the maximum mass-flow rate for each of the pumps. Observe that we have not imposed control of $\dot{m}^{\mathrm{DH}}(t)$ in (2); This mass-flow rate was implicitly calculated through the mass

balance in the Modelica model and constraints (1) and (2). To prevent the controller from charging and discharging the TES simultaneously, we imposed the concave constraint

$$\dot{m}^{\mathrm{TES-charge}}(t)\dot{m}^{\mathrm{TES-discharge}}(t) \leq \varepsilon_{\mathrm{m}}, \tag{5}$$

which corresponds to relaxation of a complementarity condition through the smoothing parameter $0 < \varepsilon_{\mathrm{m}} \ll 1$. Additionally, we have included in a similar fashion the constraint

$$\left(T^{\mathrm{TES,average}}(t) - T^{\mathrm{TES,min}}\right)\dot{m}^{\mathrm{TES-discharge}}(t) \geq -\varepsilon_{\mathrm{T}} \tag{6}$$

with $0 < \varepsilon_{\mathrm{T}} \ll 1$ to enforce that the TES should only be discharged to supply heat to the DHN when the average temperature is above a threshold value $T^{\mathrm{TES,min}}$. The necessity of this constraint arose form the number of degrees-of-freedom in the model, causing a possibility to pass water through the tank instead of the designated bypass during periods of low TES temperature.

The purpose of the TES is to minimize peak heating. As objective function, we have thus used

$$J(\bullet) = \int_{t_k}^{t_k+\Delta_t} \left(\gamma^{\mathrm{peak}} Q^{\mathrm{peak}}(t) + \gamma^{\mathrm{dump}} \sum_{i \in \mathscr{I}} Q^{\mathrm{dump},i}(t) + \sum_{j \in \mathscr{J}} \gamma^j \dot{m}^j(t)^2 + \gamma^{\mathrm{reg}} r\left(T^{\mathrm{supply}}(t), Q^{\mathrm{supply}}(t)\right) \right) \mathrm{d}t, \tag{7}$$

where the cost functional $J(\bullet)$ consists of the total peak heating, the dumped heat from boiler 5 and 6, quadratic terms on pump mass-flow rates and a regularization term

$$r\left(T^{\mathrm{supply}}(t), Q^{\mathrm{supply}}(t)\right) := \left(T^{\mathrm{supply}}(t) - \hat{T}^{\mathrm{DH}}(t)\right)^2 + \left(Q^{\mathrm{supply}}(t) - \hat{Q}^{\mathrm{DH}}(t)\right)^2. \tag{8}$$

The latter term was added to supplement the slack formulation (1) and reward supply temperatures and heat-flow rates close to the demand predictions generated from the historical data. Minimizing dumping of waste heat, in addition to peak-heating usage, favors charging of the TES as long as the boiler outlet temperature is higher than the TES temperature. This term was necessary due to the finite prediction horizon Δ_t of the MPC, which was for numerical reasons set to 36 h, beyond which the controller cannot predict a possible heat demand. The quadratic terms on the mass-flow rates minimize pump work, but these quadratic terms also served to regularize the OCP and avoid an ill-conditioned singular control problem, see Biegler [31]; Ch. 10). The cost parameters in (7) were thus set such that $\gamma^{\mathrm{peak}} \geq \gamma^{\mathrm{dump}} \gg \gamma^j > \gamma^{\mathrm{reg}}$, upon scaling of the heat and mass-flow rates.

As MPC implementation, we have used sampled-data MPC for continuous-time systems. Formulation of the OCP in continuous time allowed direction adoption and incorporation of the Modelica model of the heating plant, constituting a set of differential-algebraic equations (DAEs), into the OCP together with the constraints (1)–(6).

Remark 1. We remark that we have not in this study targeted a quantitative comparison of MPC and conventional PI control of the heating plant in sizing approaches for TES. Rather, our goal has been to assess the best possible, realizable peak-heating reduction with a TES unit, taking into account variations in the waste heat and demand, the system dynamics of the heating plant, and optimal charging and discharging of the TES. Many of the operational constraints that are included in the OCP solved by the MPC at every sample instant could, possibly, also be imposed through logics and conventional PI control. Yet, the tuning of multiple, possibly interacting decentralized PI controllers with additional logics is challenging, and often leads to more conservative operations in practice to prevent saturation of inputs and possibly detrimental oscillating effects [7]. For these reasons, MPC enables a more consistent evaluation of achievable performance with TES compared with PI control, and ensures tight satisfaction of the demand imposed from historical data.

3.3. Numerical implementation

Model development and system simulations were performed with the Modelica-based software Dymola. To implement the OCP of the heating plant, we have used the Python and Modelica-based open-source platform JModelica.org, v2.14 [35]. JModelica.org incorporates functionality to transform the infinite-dimensional OCP described in the previous section into a finite-dimensional nonlinear programming (NLP) problem using collocation on finite elements. For details on the discretization scheme, see Magnusson and Åkesson [36] or Biegler [31]; Ch. 10). To solve the resulting NLPs, we have applied the NLP solver IPOPT [37] with the MA27 linear solver [38], using the open-source software CasADI [39] for automatic differentiation. We also applied routines for symbolic elimination based on block-triangular ordering to reduce the number of algebraic variables in the NLP, which are included in the JModelica.org package [40]. Solve times of the NLP varied between 0.5 s and 2 min using a mobile workstation with an Intel Core i7-8850H CPU with 32 GB of RAM.

3.4. Evaluation metrics

To evaluate and compare the impact of different volumes for the TES tank in the heating plant, we have used as performance metrics the reduction in total peak heating and the reduction in maximum peak heating (heat-flow rate). An additional important metric is the operational flexibility and resilience against unpredicted offsets in supply and demand offered by a TES, by means of the achievable energy supply and the maximum heat-flow rate of the TES. These latter properties are commonly used as design points in TES sizing, as well as in assessment of the application of different electrical storage technologies [41]. For thermal systems with TES and varying waste heat and demand, these properties depend significantly on the governing, time-dependent and uncontrollable conditions of the waste heat, as well as the implemented control of the heating plant. To analyze this characteristic related to the sizing of a TES tank for waste-heat utilization in DH, we have evaluated the distribution of energy supply (E) and heat-flow rate (Q) for each discharging period $k \in \mathscr{T}^{\mathrm{dc}}$ and considered TES volume $v \in \mathscr{V}^{\mathrm{TES}}$, as

well as the associated energy-to-heat-flow ratio E/Q^{vk} for each discharging period, defined as

$$E \Big/ Q^{vk} := \frac{\int_{t'}^{t'+\Delta_k^{dc}} Q^{\text{TES-discharge}}(t)dt}{\max_{t\in[t',t'+\Delta_k^{dc}]} Q^{\text{TES-discharge}}(t)}, \quad (9)$$

where t' is the onset time and Δ_k^{dc} the length of discharging period k, and $Q^{\text{TES-discharge}}(t)$ the heat-flow rate from the tank. The E/Q ratio is a trade off in all energy storage, and provides a constructive metric for comparing the utilization of different volumes of the TES tank relative to the waste-heat availability and the heat demand.

4. Results

The sizing of a TES for the heating plant of Mo District Heating was evaluated with the proposed methodology using seven different TES volumes over the aforementioned 6-month evaluation period from November 2018 through April 2019. From initial screening of the data, the tank volumes were selected to be in the range from 500 to 3500 m^3 with equal spacing, i.e. $\mathscr{V}^{\text{TES}} = \{500, 1000, \ldots, 3500\}$. In addition, the dynamic system model of the heating plant without TES was optimized with the proposed MPC scheme. For the predictions of available waste heat $\hat{Q}^{\text{WH},i}$, heat demand $\hat{Q}^{\text{DH}}$ and return temperature $\hat{T}^{\text{return}}$ supplied to the MPC controller, we have used the actual historical time series and thus assumed perfect predictions. The prediction horizon of the MPC was $\Delta_t = 36$ h and the sampling time $\delta = 2$ h. For the slack constraints (1), we have used $\alpha = 2.5$°C and $\beta = 0.03$.

Fig. 6 shows parity plots of (a) the required vs. simulated supply temperature, and (b) required vs. simulated heat delivered to the DHN for the different TES tank volumes in the set $\mathscr{V}^{\text{TES}}$. All displayed simulation values were obtained from post-simulations (Step 3 in Fig. 4) with optimized control inputs (from Step 2 in Fig. 4). Except for a single sample for $V^{\text{TES}} = 500$ m^3, the simulated supply temperature samples are for all the seven TES volumes within the imposed bounds (1a). Fig. 6b shows that the corresponding samples of the simulated heat-flow rate $Q^{\text{supply}}(t)$ to the DHN, relative to the required heat-supply $Q^{\text{DH}}(t)$, are within the cone arising from the added upper slack β in constraint (1b). A few samples of $Q^{\text{supply}}(t)$ for the case with $V^{\text{TES}} = 2500$ m^3 can be seen in Fig. 6b to violate the lower bound in (1b). Notwithstanding, the correlation coefficient between the data and the simulations in Fig. 6b is greater than 0.99 for all cases, confirming that the few observed deviations in the heat supply were insignificant.

Fig. 7 shows load-duration curves for peak heating with the different TES tank volumes for the considered 6-month period. It can be observed that peak-heating demands above 10 MW are almost identical for all cases. This is due to the fact that these demands occurred during the coldest periods when all waste heat was directly utilized. The TES tank could therefore not be charged as no additional waste heat from the ferrosilicon plant was available. Fig. 7 further shows that even the smallest tank reduces the number of hours with peak heating significantly compared with the base case. The accumulated peak-heating usage is listed in Table 2,

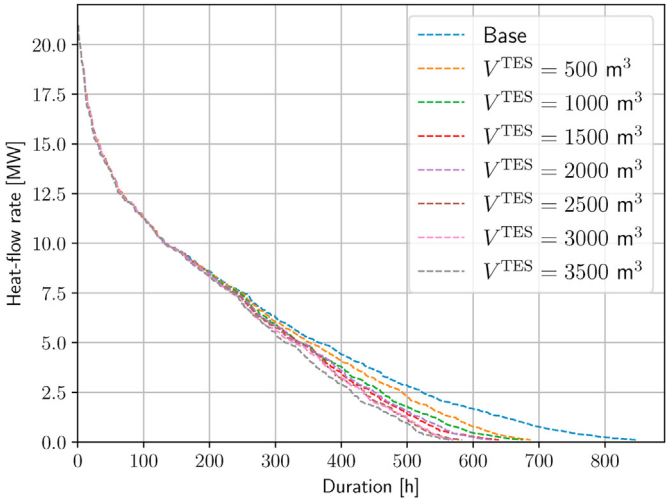

Fig. 7. Peak-heating load-duration curves for different TES tank volumes and base case.

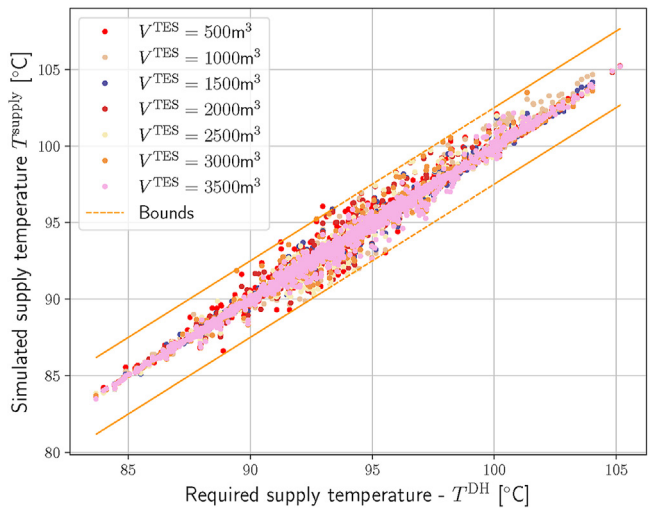

(a) Supply temperature.

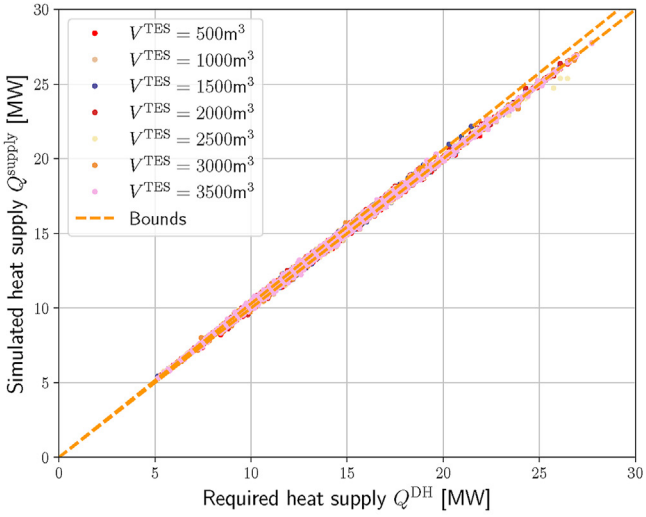

(b) Heat supply.

Fig. 6. Parity plots of (a) the DH supply temperature and (b) the delivered heat to DHN, comparing simulations with optimized control inputs obtained from the MPC controller and corresponding values from the base-case simulations in Step 1 of Fig. 4, using plant measurement data. The bounds given by constraints (1a) and (1b), respectively, are shown in yellow lines. (For interpretation of the references to colour in this figure legend, the reader is referred to the Web version of this article.)

Table 2
Accumulated results for the total considered 6-month period $E^{\text{TES,eval}}$ from November 2018 through April 2019.

TES Volume [m^3]	Base (0)	500	1000	1500	2000	2500	3000	3500
Total peak heating [MWh]	8846	8303	7980	7784	7828	7617	7563	7372
Peak heating savings to base [%]	0	6.1	9.8	12.0	11.5	13.9	14.5	16.7

which shows that the relative reduction ranged from 6.1 to 16.7%.

The available waste heat from the ferrosilicon plant, the operating conditions of the heating plant, and the weather conditions varied significantly during the considered evaluation period. To elaborate on the impact of these variations, we have in Fig. 8 decomposed the reduction in peak heating on a monthly basis. The displayed results are relative peak-heating consumption per month compared to the base case, i.e., without TES. The effective reduction in peak heating per volume for the different months varies greatly, particularly for the larger considered tank volumes, and does not exhibit a linear trend with increasing volume. For November 2018, the TES with volume 3500 m^3 gave more than twice as high peak-heating reduction compared with a volume of 3000 m^3, while for December 2018 the three largest volumes eliminated almost all the peak heating. For the first two months of 2019, it can be seen from Fig. 3 that little heat was dumped and as such, limited additional waste heat could be utilized. Consequently, none of the TES tank volumes were able to reduce the peak heating for this month. In March 2019, there were subsequent, relatively short periods of heat dumping and peak-heating demand. For this month, the differences in peak-heating reduction for different TES tank volumes were relatively small compared with December and April. Comparing with Fig. 3, it can be seen that the first week of March had a period with large peak-heating demand and no dumped heat, causing only a 20–30% peak-heating reduction for all the considered TES tank volumes for this month. For April 2019, the largest TES tank volume of 3500 m^3 eliminated all peak heating, while a volume of 500 m^3 was inferior compared with the other considered tank volumes.

In Fig. 9, we show the relative maximum peak heating per month. For November 2018, none of the TES volumes were able to reduce the large maximum peak heating of up to 10 MW lasting for several days towards the end of the month, cf. Fig. 3. December 18 had relatively low peaks in the demand, and consecutive periods with heat dumping and peak heating. With such pattern, TES could potentially eliminate a significant share of the necessary peak heating. Interestingly, the case with TES tank volume of 2500 m^3 and 3000 m^3 were more effective in reducing the maximum peak

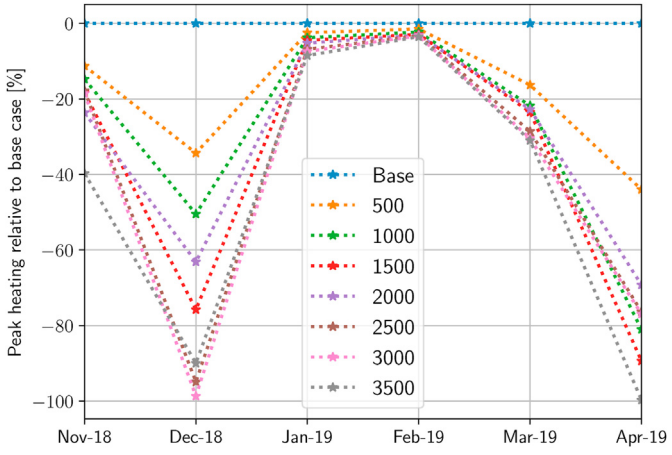

Fig. 8. Relative monthly peak-heating usage compared with base case, i.e. with no TES.

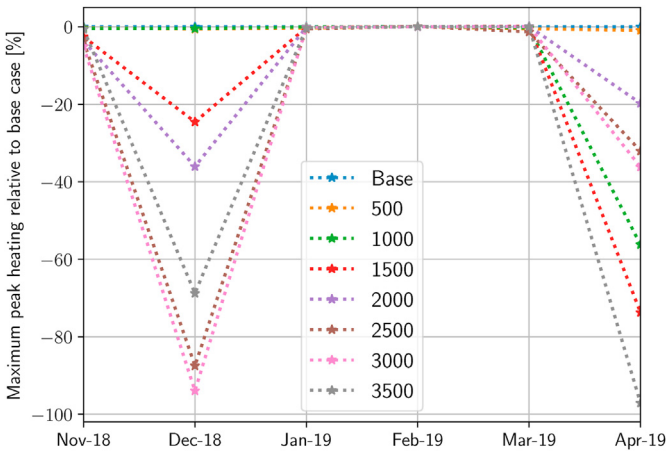

Fig. 9. Relative maximum peak heating per month compared with base case, i.e. with no TES.

heating than the case with 3500 m^3. This is a result of reduced charging times of the tanks with lower volumes. Comparing with the total monthly peak-heating reduction in Fig. 8, these two volumes were the most effective for peak-heating reduction in December 2018. Too low TES volumes, as seen by the case with 500 m^3 and 1000 m^3, caused too little capacity of the TES to be effective in this month. For the months of January–March 2019, none of the different TES volumes were able to reduce the maximum peak heating. Even though we supplied the MPC with perfect load and waste-heat predictions, the maximum peaks occur after periods with no or insufficient amounts of dumped heat that could be pre-charged to the TES. Finally, for the last considered month, April 2019, the TES with volume 1000 m^3 and 1500 m^3 gave more effective reduction of the maximum peak heating appearing at beginning of the month than the larger volumes, except for the largest volume of 3500 m^3. This underpins the challenge of optimal sizing of TES tanks in presence of large temperature and heat-flow variations in the utilized waste heat.

Fig. 10 shows a boxplot of the E/Q ratio as defined in (9) for each heat discharging period $k \in \mathscr{T}^{\text{dc}}$ and TES tank volume $v \in \mathscr{V}^{\text{TES}}$. Corresponding boxplots of the discharged energy and maximum heat-flow rate for each discharging period are shown in Fig. 11. The orange line shows the median value, the boxes represent the inter-quartile range (i.e. 50 % score), and the circles the 0.7% outliers. The median E/Q ratio increases notably with increasing volume up to 2000 m^3. The highest E/Q ratio, as well as the highest median energy supply (Fig. 11a) and the highest median heat-flow rate (Fig. 11b), is achieved for the TES tank with a volume of 3000 m^3. The TES tank volumes in the range 1500–3000 m^3 have a rather similar distribution of the E/Q ratio, with the inter-quartile range for 3000 m^3 being slightly higher. The highest outlier values of the E/Q ratios exhibit a close to linear trend with increasing TES tank volume, and the same observation can been drawn for the distribution of energy supply from the TES shown in Fig. 11a. Generally, both the E/Q ratio, energy and heat-flow rate per discharging period are more scattered for the two smallest volumes. This indicates a less precise characterization of the actual energy, heat-

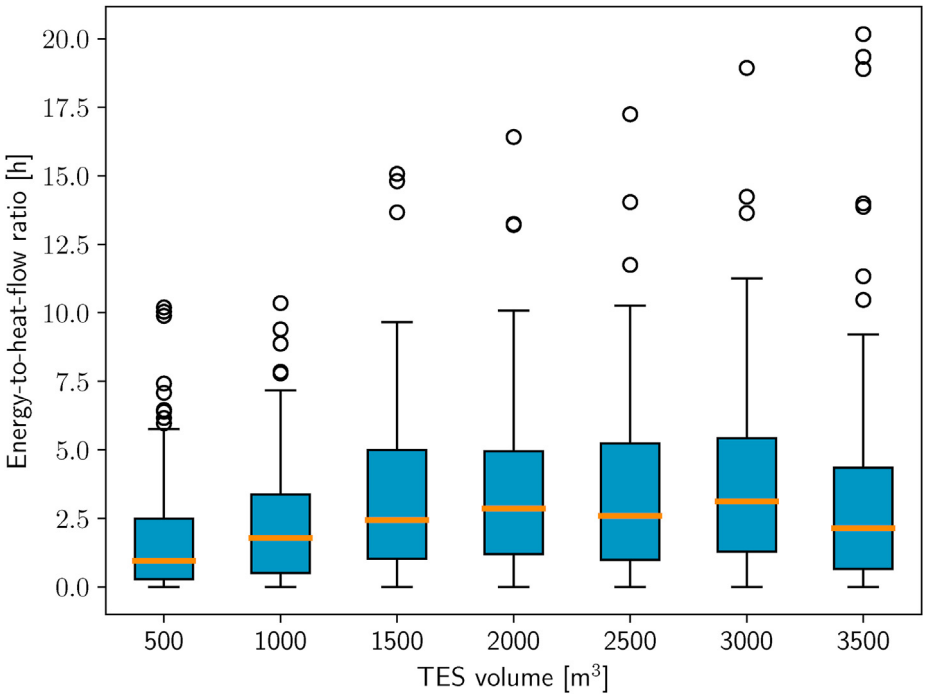

Fig. 10. Energy-to-heat-flow (E/Q) ratio as defined in (9) for different TES tank volumes.

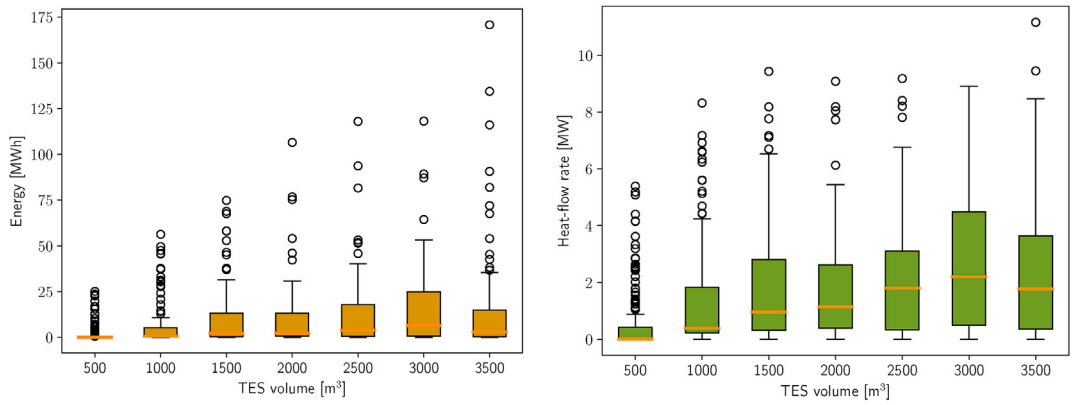

(a) Energy. (b) Maximum heat-flow rate

Fig. 11. (a) Delivered energy and (b) maximum heat-flow rate from the TES during each discharging period for different TES tank volumes.

flow rate and associated ratio these smaller tank volumes can provide, i.e. there is larger uncertainty of the E/Q ratio of these TES tank volumes.

Judging from the reduction in peak-heating energy consumption and reduction in maximum peak heating shown in Figs. 8 and 9, respectively, a TES tank volume of 1500 m^3 would be a good choice. Larger tank volumes gave higher reductions in the maximum peak heating. However, the implemented MPC formulation minimized energy usage and not the maximum peak; replacing or modifying the chosen cost function (7) with penalization of maximum peak heating could change this observation. Based on the energy supplied in each discharging period, the maximum heat-flow rate and the corresponding E/Q ratio for the different TES tank volumes, a volume of 3000 m^3 exhibited the overall best performance. For these performance metrics, a volume of 1500 m^3 again gave good performance, and little is gained from increasing the volume to 2000–2500 m^3. The largest considered tank volume, 3500 m^3, still offers the largest total energy saving, and the single largest value of supplied energy, maximum heat-flow rate, and maximum E/Q ratio. In some case, these could all be desirable design criteria, while the higher cost and associated payback period of large hot-water tanks will for most cases not justify such large volume. The recommended tank volume of 1500 m^3 for the Mo District Heating case study is in the same order as the result in the study by Ref. [10] based on a related case study with economic evaluation of different tank volumes under different mixes of peak heating.

5. Discussion

The optimal size of a TES in heating plants is always a trade-off between costs, available space, and the desired functionality of the storage with respect to variations in the waste-heat availability and the demand. Fully accounting for the impact of variations in the

residual heat in sizing of a TES requires dynamic modeling of the heating plant and considering the control of the system. The proposed use of MPC provides a means of incorporating the performance gain from optimal control in assessment of different storage sizes. Also, it ensures that the heating-plant simulations comply with the historical demand data as shown in Fig. 6. The varying and often uncertain waste-heat availability makes it challenging to identify a single, optimal tank volume for a heating plant. As an alternative approach, the sizing methodology used in the paper enables confidently analyzing different TES volumes for the trade-off between peak-heating reduction and desired E/Q-ratio. Hence, the presented methodology may be useful in decision making for implementation of TES on a case to case basis, and thus support decarbonization efforts and increased waste-heat utilization in heat supply both to the residential [42] and commercial [19] building sectors in many countries.

One of the merits of the proposed approach compared with optimization approaches based on selection of representative days, such as in van der Heijde et al. [43]; is the ability to evaluate and optimize the size of a TES over both a long time horizon and with sufficiently short time steps to capture the governing heating-plant dynamics. Combining dynamic system simulations and analysis of energy supply, heat-flow rate and the associated E/Q ratio for each discharge period provides valuable insights in performance trade-offs of different TES tank volumes. Compared with the approach in Pinnau and Breitkopf [13]; where an inverse measure of (9) was applied but with energy balances only and no consideration of temperature variations, the proposed approach enables evaluations of the energy and thermal-power capacities of the TES taking into account the impact of temperature variations in the storage, the waste heat, and the flow to the DHN. Using this approach, the analysis clearly showed that a comparably low tank volume would be a good choice with respect to peak-heating reduction and the E/Q-ratio.

We have in this study not targeted a quantitative comparison of different control solutions or control objectives, nor the effect of discrepancies in the predicted and actual demand. As stated in Remark 1, significant tuning would be required to achieve a comparable performance as the MPC with use of conventional PI control. Moreover, the same satisfaction of demand as the constraint formulation (1) offers cannot in general be guaranteed. Thus it is more challenging to ensure a fair performance comparison with and without TES using historic plant data.

The conducted case study was based on a selected 6-month period, and we have assumed perfect predictions in the MPC as a means of assessing the maximum achievable peak-heating reduction with optimal control of the heating plant and different TES tank volumes. As the heat production is a slow process and the MPC re-optimizes the control inputs on a receding horizon, imperfect demand and waste-heat predictions would to a large extent be recovered by the feedback and updates of these predictions at each sampling instant. We have also based the study on the use of a single TES tank; there may be scenarios for waste-heat availability and given heating-plant configuration where using two or more smaller TES tanks could be a better option. This, as well as a multiple-scenario approach for waste-heat availability and demand, is a topic for further work.

6. Conclusions

This paper has presented a combined dynamic simulation and optimization based methodology for the sizing of TES in a DH plant. The methodology accounts for the key dynamics of the heating plant with TES, the effect of optimal control, and the time variations of the waste heat and the heat demand. The applied MPC approach constitutes a numerically tractable means of incorporating optimal control in the evaluation of different TES tank volumes over long time horizons. Together with the proposed E/Q metric for evaluating the heat-discharging properties of the TES tank as a function of tank volume, the proposed methodology allows an assessment of both the total peak-heating reduction and the added resilience against unpredictable variations in supply and demand with different TES tank volumes. For the considered case study, with an annual heat production of 85–90 GWh of which about 90% comes from the off-gas waste heat, a 12% effective peak-heating reduction and a median E/Q ratio of 2.5 h over the six month period was achieved with a volume of 1500 m^3. The final economical and environmental benefits of integrating a TES tank into a heating plant depend on the plant's peak heating sources and thus cannot be generalized.

Credit roles

Brage Rugstad Knudsen: Conceptualization, Methodology, Software, Formal analysis, Investigation, Writing – original draft, Funding acquisition; Daniel Rohde: Conceptualization, Methodology, Software, Formal analysis, Validation, Writing – review & editing; Hanne Kauko: Conceptualization, Validation, Formal analysis, Writing – review & editing, Funding acquisition, Project administration.

Declaration of competing interest

The authors declare that they have no known competing financial interests or personal relationships that could have appeared to influence the work reported in this paper.

Acknowledgements

This study has been partly funded by HighEFF - Centre for an Energy Efficient and Competitive Industry for the Future under the FME-scheme (Centre for Environment-friendly Energy Research, 257632), and partly by LTTG + - Low-temperature thermal grids with surplus heat utilization (Knowledge Building Project 280994). The authors gratefully acknowledge the financial support from the Research Council of Norway and the user partners of HighEFF and LTTG+. Furthermore, the authors thank Jørn Hanssen and Terje Sund-Olsen at Mo Fjernvarme for providing data and information about the case study, and Johannes Jäschke and Mandar Thombre at NTNU for helpful discussions.

References

[1] Wheatcroft E, Wynn H, Lygnerud K, Bonvicini G, Leonte D. The role of low temperature waste heat recovery in achieving 2050 goals: a policy positioning paper. Energies 2020;13(8):2107.
[2] Miró L, Brückner S, Cabeza LF. Mapping and discussing industrial waste heat (IWH) potentials for different countries. Renew Sustain Energy Rev 2015;51:847–55.
[3] Persson U, Möller B, Werner S. Heat roadmap europe: identifying strategic heat synergy regions. Energy Pol 2014;74:663–81.
[4] Olsthoorn D, Haghighat F, Mirzaei PA. Integration of storage and renewable energy into district heating systems: a review of modelling and optimization. Sol Energy 2016;136:49–64.
[5] Guelpa E, Verda V. Thermal energy storage in district heating and cooling systems: a review. Appl Energy 2019;252:113474.
[6] Martínez-Lera S, Ballester J, Martínez-Lera J. Analysis and sizing of thermal energy storage in combined heating, cooling and power plants for buildings. Appl Energy 2013;106:127–42.
[7] Birk W, Atta KT, Uden F. Improving district heating system operation through control configuration selection and adaptive control. In: European control conference; 2019. p. 2944–9.
[8] Cao M, Cao J. Optimal design of thermal-energy stores for boiler plants. Appl Energy 2006;83:55–68.
[9] Labidi M, Eynard J, Faugeroux O. Optimal design of thermal storage tanks for

multi-energy district boilers. In: 4th inverse problems, design and optimization symposium (IPDO-2013); 2013.
[10] Kauko H, Rohde D, Knudsen BR, Sund-Olsen T. Potential of thermal energy storage for a district heating system utilizing industrial waste heat. Energies 2020;13:3923.
[11] Badami M, Fonti A, Carpignano A, Grosso D. Design of district heating networks through an integrated thermo-fluid dynamics and reliability modelling approach. Energy 2018;144:826–38.
[12] Kyriakis SA, Younger PL. Towards the increased utilisation of geothermal energy in a district heating network through the use of a heat storage. Applied Thermal Engingeering 2016;94:99–110.
[13] Pinnau S, Breitkopf C. Determination of Thermal Energy Storage (TES) characteristics by Fourier analysis of heat load profiles. Energy Convers Manag 2015;101:343–51.
[14] Stalinski D, Duquette J. Development of a simplified method for optimally sizing hot water storage tanks subject to short-term intermittent charge/discharge cycles. Journal of Energy Storage 2021;37:102463.
[15] Caliano M, Bianco N, Graditi G, Mongibello L. Design optimization and sensitivity analysis of a biomass-fired combined cooling, heating and power system with thermal energy storage systems. Energy Convers Manag 2017;149:631–45.
[16] Sartor K, Dewallef P. Integration of heat storage system into district heating networks fed by a biomass CHP plant. Journal of Energy Storage 2018;15:350–8.
[17] Urbanucci L, D'Ettorre F, Testi D. A comprehensive methodology for the integrated optimal sizing and operation of cogeneration systems with thermal energy storage. Energies 2019;12(5).
[18] Pérez-Iribarren E, González-Pino I, Azkorra-Larrinaga Z, Gómez-Arriarán I. Optimal design and operation of thermal energy storage systems in micro-cogeneration plants. Appl Energy 2020;265:114769.
[19] Simeoni P, Ciotti G, Cottes M, Meneghetti A. Integrating industrial waste heat recovery into sustainable smart energy systems. Energy 2019;175:941–51.
[20] Simeoni P, Nardin G, Ciotti G. Planning and design of sustainable smart multi energy systems. The case of a food industrial district in Italy. Energy 2018;163:443–56.
[21] Li H, Hou J, Hong T, Ding Y, Nord N. Energy, economic, and environmental analysis of integration of thermal energy storage into district heating systems using waste heat from data centres. Energy 2021;219:119582.
[22] Alnaser SW, Member GS, Ochoa LF, Member S. Optimal sizing and control of energy storage in wind power-rich distribution networks. IEEE Trans Power Syst 2016;31(3):2004–13.
[23] Das CK, Bass O, Kothapalli G, Mahmoud TS, Habibi D. Overview of energy storage systems in distribution networks: placement, sizing, operation, and power quality. Renew Sustain Energy Rev 2018;91:1205–30.
[24] Tarragona J, de Gracia A, Cabeza LF. Bibliometric analysis of smart control applications in thermal energy storage systems. A model predictive control approach. Journal of Energy Storage 2020;32:101704.
[25] Jonin M, Khosravi M, Eichler A, Schuetz P, Jones CN, Smith RS. Exergy-based model predictive control for design and control of a seasonal thermal energy storage system. In: J. Phys.: conf. Ser; 2019. p. 1343.
[26] D'Ettorre F, Conti P, Schito E, Testi D. Model predictive control of a hybrid heat pump system and impact of the prediction horizon on cost-saving potential and optimal storage capacity. Appl Therm Eng 2019;148:524–35.
[27] Thombre Mandar, Prakash Sandeep, Knudsen Brage Rugstad, Jäschke Johannes. Optimizing the Capacity of Thermal Energy Storage in Industrial Clusters. In: Pierucci Sauro, Manenti Flavio, Luisa Bozzano Giulia, Manca Davide, editors. 30th European Symposium on Computer Aided Chemical Engineering, 48. Elsevier; 2020. p. 1459–64.
[28] Fritzson P, Bunus P. Modelica - a general object-oriented language for continuous and discrete-event system modeling and simulation. In: Proc. 35th annual simulation symposium, 2002. San deigo, CA, USA; 2002.
[29] Schweiger G, Larsson P-O, Magnusson F, Lauenburg P, Velut S. District heating and cooling systems – framework for Modelica-based simulation and dynamic optimization. Energy 2017;137:566–78.
[30] Incropera FP, DeWitt DP, Bergman TL, Lavine AS. Heat exchangers, book section 11. John Wiley & Sons; 2007.
[31] Biegler LT. Nonlinear programming: concepts, algorithms, and applications to chemical processes. Philadelphia, PA: SIAM; 2010.
[32] Geysen D, De Somer O, Johansson C, Brage J, Vanhoudt D. Operational thermal load forecasting in district heating networks using machine learning and expert advice. Energy Build 2018;162:144–53.
[33] Guelpa E, Marincioni L, Capone M, Deputato S, Verda V. Thermal load prediction in district heating systems. Energy 2019;176:693–703.
[34] Knudsen BR, Kauko H, Andresen T. An optimal-control scheme for coordinated surplus-heat exchange in industry clusters. Energies 2019;12(10).
[35] Åkesson J, Årzén KE, Gäfvert M, Bergdahl T, Tummescheit H. Modeling and optimization with Optimica and JModelica.org-Languages and tools for solving large-scale dynamic optimization problems. Comput Chem Eng 2010;34(11):1737–49.
[36] Magnusson F, Åkesson J. Collocation methods for optimization in a Modelica environment. In: Proc. Of the 9th international Modelica conference; 2012. p. 649–58.
[37] Wächter A, Biegler LT. On the implementation of an interior-point filter line-search algorithm for large-scale nonlinear programming. Math Program apr 2005;106(1):25–57.
[38] HSL. A collection of fortran codes for large scale scientific computation. 2018. www.hsl.rl.ac.uk, accessed 03/2018.
[39] Andersson JAE, Gillis J, Horn G, Rawlings JB, Diehl M. CasADi: a software framework for nonlinear optimization and optimal control. Mathematical Programming Computation 2018;11:1–36.
[40] Magnusson F, Åkesson J. Symbolic elimination in dynamic optimization based on block-triangular ordering. Optim Methods Software 2018;33(1):92–119.
[41] Zerrahn A, Schill WP. Long-run power storage requirements for high shares of renewables: review and a new model. Renew Sustain Energy Rev 2017;79:1518–34.
[42] Ma M, Ma X, Cai W, Cai W. Carbon-dioxide mitigation in the residential building sector: a household scale-based assessment. Energy Convers Manag 2019;198:111915.
[43] van der Heijde B, Vandermeulen A, Salenbien R, Helsen L. Representative days selection for district energy system optimisation: a solar district heating system with seasonal storage. Appl Energy 2019;248:79–94.